Detecting binary neutron star systems with spin in advanced gravitational-wave detectors.

Duncan A. Brown,[1] Ian Harry,[1] Andrew Lundgren,[2,3] and Alexander H. Nitz[1]

[1]*Department of Physics, Syracuse University, Syracuse NY 13244*
[2]*Institute for Gravitation and the Cosmos, The Pennsylvania State University, University Park, PA 16802*
[3]*Albert-Einstein-Institut, Callinstr. 38, 30167 Hannover, Germany*

The detection of gravitational waves from binary neutron stars is a major goal of the gravitational-wave observatories Advanced LIGO and Advanced Virgo. Previous searches for binary neutron stars with LIGO and Virgo neglected the component stars' angular momentum (spin). We demonstrate that neglecting spin in matched-filter searches causes advanced detectors to lose more than 3% of the possible signal-to-noise ratio for 59% (6%) of sources, assuming that neutron star dimensionless spins, $c\mathbf{J}/GM^2$, are uniformly distributed with magnitudes between 0 and 0.4 (0.05) and that the neutron stars have isotropically distributed spin orientations. We present a new method for constructing template banks for gravitational wave searches for systems with spin. We present a new metric in a parameter space in which the template placement metric is globally flat. This new method can create template banks of signals with non-zero spins that are (anti-)aligned with the orbital angular momentum. We show that this search loses more than 3% of the maximum signal-to-noise for only 9% (0.2%) of BNS sources with dimensionless spins between 0 and 0.4 (0.05) and isotropic spin orientations. Use of this template bank will prevent selection bias in gravitational-wave searches and allow a more accurate exploration of the distribution of spins in binary neutron stars.

I. INTRODUCTION

The second-generation gravitational wave detectors Advanced LIGO (aLIGO) and Advanced Virgo (AdV) [1, 2] are expected to begin observations in 2015, and to reach full sensitivity by 2018-19. These detectors will observe a volume of the universe more than a thousand times greater than first-generation detectors and establish the new field of gravitational-wave astronomy. Estimated detection rates for aLIGO and AdV suggest that binary neutron stars (BNS) will be the most numerous source detected, with plausible rates of $\sim 40/\text{yr}$ [3]. Gravitational wave observations of BNS systems will allow measurement of the properties of neutron stars and allow us to explore the processes of stellar evolution.

The gravitational waves that advanced detectors will observe from inspiralling BNS systems are well described by post-Newtonian theory [4]. As the neutron stars orbit each other, they lose energy to gravitational waves causing them to spiral together and eventually merge. If the angular momentum (spin) of the component neutron stars is zero, the gravitational waveform emitted depends at leading order on the chirp mass of the binary $\mathcal{M} = (m_1 m_2)^{3/5} / (m_1 + m_2)^{1/5}$ [5], where m_1, m_2 are the component masses of the two neutron stars, and at higher order on the symmetric mass ratio $\eta = m_1 m_2 / (m_1 + m_2)^2$ [6–11]. If the neutron stars are rotating, coupling between the neutron stars' spin $\boldsymbol{S}_{1,2}$ and the orbital angular momentum $\boldsymbol{L}$ of the binary will affect the dynamics of BNS mergers [12–15]. We measure the neutron stars' spin using the dimensionless parameter $\boldsymbol{\chi}_{1,2} = \boldsymbol{S}_{1,2}/m_{1,2}^2$.

The maximum spin value for a wide class of neutron star equations of state is $\chi \equiv |\boldsymbol{\chi}| \sim 0.7$ [16]. However, the spins of neutron stars in BNS systems is likely to be smaller than this limit. The spin period at the birth of a neutron star is thought to be in the range 10–140 ms [17, 18]. During the evolution of the binary, accretion may increase the spin of one of the stars [19], however neutron stars are unlikely to have

periods less than 1 ms [20], corresponding to a dimensionless spin of $\chi \sim 0.4$. The period of the fastest known pulsar in a double neutron star system, J0737–3039A, is 22.70 ms [21], corresponding to a spin of only $\chi \sim 0.05$. In this paper, we therefore consider two populations of neutron star binaries: the first has spins uniformly distributed from $\chi = 0$ to 0.4, the second, a sub-set of this, has spins between 0 and 0.05. This extended spin distribution allows for the possibility of serendipitous discovery of BNS systems in globular clusters, where the evolutionary paths may be different than that in field binaries [22]. Since supernova kicks may cause the direction of the neutron star's angular momentum to be misaligned with the orbital angular momentum of the binary [23], or the binaries may be formed by direct capture, we consider a population of binaries with an isotropic spin distribution.

Searches for binary neutron star systems in gravitational-wave detectors use template-based searches [24]. Data from the detector is correlated against a bank of known template waveforms, which cover the space of parameters searched over [25]. The template bank is constructed so that it covers the parameter space of interest so that any signal in this region will lose no more than 3% of the signal-to-noise ratio obtained by an exactly matching template. Alternative search methods have been proposed [26, 27], however these still require the construction of a template bank to perform the search. The effect of spin-orbit and spin-spin interactions were neglected in previous BNS searches [28], as they do not have a significant effect on the ~ 1600 gravitational wave cycles in the 40–2000 Hz sensitive band of first-generation detectors [29]. However, aLIGO and AdV will be sensitive to gravitational-wave frequencies between 10–2000Hz, increasing the number of cycles in band by an order of magnitude. Initial studies have demonstrated that over this band, the small secular effects produced by spin-orbit and spin-spin coupling will have a significant effect on the detectability of BNS systems with non-trivial component spins [30]. However, the current ge-

ometric method for placing BNS templates [31] does not incorporate spin. While numerical (stochastic) methods could be used to include spin, these require substantially more templates than a comparable geometric approach [32].

We present a new geometric algorithm for placing templates for BNS systems with spin, which has a significantly higher sensitivity than previous searches. Our new algorithm constructs a metric on the parameter space using the various coefficients of the TaylorF2 expansion of the orbital phase as coordinates. In such a coordinate system the parameter space metric is globally flat, therefore we can transform into a Euclidean coordinate system. Finally, our method uses a Principal Coordinate Analysis to identify a two dimensional manifold that can be used to cover the aligned spin BNS parameter space using existing two dimensional lattice placement algorithms.

To demonstrate our new method, we first perform a systematic evaluation of the ability of a search that neglects spin to detect gravitational waves for BNS in aLIGO and AdV. We show that this search will lose more than 3% of the matched filter signal-to-noise ratio for 59% (6%) of signals if it is used to search for BNS systems with spins uniformly distributed between $0 \leq \chi_{1,2} \leq 0.4(0.05)$; this is unsatisfactory over a large region of the signal parameter space. We show that by considering BNS systems where the spin of the neutron stars are aligned with the orbital angular momentum (i.e. the binary is not precessing), we can create a two-dimensional template bank that is efficient at detecting spin-aligned BNS signals. Finally we demonstrate that this bank is sufficient to detect signals from generic spinning, precessing binaries in aLIGO and AdV. The spin-aligned bank loses more than 3% of the signal-to-noise ratio for only 9% (0.2%) of signals, sufficient to construct a sensitive and unbiased search for BNS systems in aLIGO and AdV.

II. BNS SEARCH SENSITIVITY

We quantify the performance of templated matched-filter searches by the fitting factor (FF) of the search [33]. The fitting factor is the fraction of the signal-to-noise ratio that would be recovered when matching a given signal with the best matching waveform in the template bank. We first define the overlap between two templates h_1 and h_2 as

$$\mathcal{O}(h_1, h_2) = (\hat{h}_1 | \hat{h}_2) = \frac{(h_1 | h_2)}{\sqrt{(h_1 | h_1)(h_2 | h_2)}}. \qquad (1)$$

which is defined in terms of the noise-weighted inner product [34]

$$(h_1 | h_2) = 4 \, \text{Re} \int_0^\infty \frac{\tilde{h}_1(f) \tilde{h}_2^*(f)}{S_n(f)} df. \qquad (2)$$

This overlap is the fraction of signal power that would be recovered by searching for the signal h_1 using a matched filter constructed from h_2. Maximizing the overlap over the time of arrival and waveform phase yields the match

$$\mathcal{M}(h_1, h_2) = \max_{\phi_c, t_c} (\hat{h}_1 | \hat{h}_2(\phi_c, t_c)). \qquad (3)$$

The mismatch, $1 - \mathcal{M}$, is the fraction of the optimal signal-to-noise ratio that is lost when searching for a signal h_1 with a template waveform h_2.

When searching for BNSs, we do not know the exact physical parameters of the system. We assume that the masses of the neutron stars lie between 1 and $3 \, M_\odot$ and construct a bank of waveform templates $\{h_b\}$ to span this region of the mass parameter space. To measure the sensitivity of this bank to a gravitational waveform h_s with unknown parameters, we compute the fitting factor

$$\text{FF}(h_s) = \max_{h \in \{h_b\}} \mathcal{M}(h_s, h), \qquad (4)$$

where we have maximized the match over all the templates in the bank. In searches for gravitational waves using LIGO and Virgo, the bank is constructed such that the fitting factor for any signal in the target parameter space will never be less than 0.97. At least one of the templates in the bank must have a maximized overlap of 0.97 (or more) with the signal. This value is chosen to correspond to an event rate loss of no more than 10% of possible sources within the range of the detectors [35]. In this paper, we use a fitting factor of 0.97 to construct search template banks.

We now test whether a bank of templates that does not model the effect of spin is sufficient to detect generic, spinning BNS sources in aLIGO and AdV. We create a bank of non-spinning templates that would recover any non-spinning BNS system with a fitting factor greater than 0.97. This bank is constructed using TaylorF2 waveforms, which are constructed using the stationary phase approximation to the gravitational-wave phasing accurate to 3.5 post-Newtonian (PN) order [4, 36]. To create a bank of these waveforms we use the hexagonal-placement method defined in [37], which was used in the majority of previous searches in LIGO and Virgo [38–40]. This template bank is placed using the metric given in [25], which is valid, by construction, for templates at 2PN order. Our signal waveforms are constructed using the SpinTaylorT4 waveform [41], a time-domain waveform accurate to 3.5PN order in the orbital phase which includes the leading order spin-orbit, spin-spin, and precessional modulation effects and implemented in the LSC Algorithm Library Suite [42]. We first confirm that although the bank is constructed at 2PN order, it yields fitting factors greater than 0.97 for both the TaylorF2 and SpinTaylorT4 non-spinning waveforms at 3.5PN order. To simulate a population of spinning BNS sources, we generate 100,000 signals with component masses uniformly distributed between 1 and $3 \, M_\odot$ and dimensionless spin magnitudes uniformly distributed between 0 and 0.4. The orientation of the spin, the orientation of the orbital angular momentum, and the sky location are isotropically distributed. To model the sensitivity of a second generation gravitational wave interferometer, we use the aLIGO zero-detuned, high-power sensitivity curve [43]. For our simulations, we use a lower frequency cutoff of 15Hz.

We note that for non-precessing systems the fitting factor is independent of the detector alignment and location; however this statement is not true for precessing systems. For such systems, however, the distribution of fitting factors over a population of sources will be independent of the detector alignment
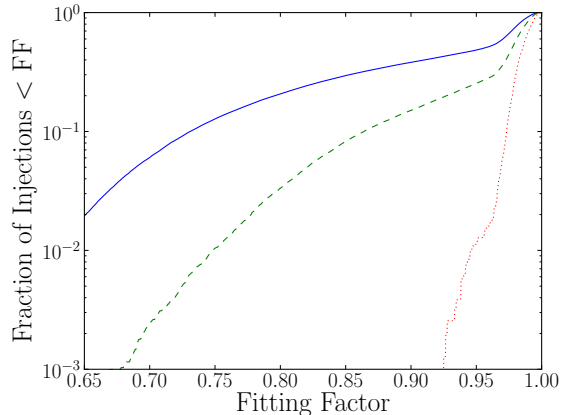
FIG. 1. The distribution of fitting factors obtained by searching for the precessing BNS systems described in section II with component spins up to 0.4 (blue solid line), 0.2 (green dashed line), and 0.05 (red dotted line) using the non-spinning BNS template bank described in section II and the advanced LIGO, zero-detuned, high-power PSD with a 15Hz lower frequency cutoff.

and location. Therefore, for this study we calculate the fitting-factor for a single detector with an arbitrary location and position.

In Fig. 1 we show the distribution of fitting factors obtained when searching for our population of BNS sources with the non-spinning template bank. We see that 59% of signals were recovered with a fitting factor less than 0.97. If the maximum spin magnitude is restricted to 0.05, we find that 6% of signals are recovered with a FF less than 0.97. If BNS systems do exist with spin magnitudes up to 0.4, a template bank that captures the effects of spin will be required to maximize the number of BNS detections. Detection efficiency will be greatly reduced by using a template bank that only contains waveforms with no spin effects. Even under the assumption that component spins in BNS systems will be no greater than 0.05, detection efficiency will be decreased if the effect of spin on the signal waveform is ignored.

III.   A TEMPLATE PLACEMENT ALGORITHM FOR ALIGNED-SPIN BNS TEMPLATES

As we have demonstrated in the previous section, there is a substantial region of the BNS parameter space where a significant loss in signal-to-noise ratio would be encountered when searching for astrophysically plausible, spinning BNS systems with non-spinning templates. It has been suggested that using BNS templates where the spins of the system are aligned with the orbital angular momentum is sufficient for detecting generic BNS systems with second-generation detectors [30] using TaylorF2 templates that incorporate the leading order spin-orbit and spin-spin corrections [44].

In this section we use these spin-aligned waveforms to construct a template bank that attempts to cover the full space of astrophysically plausible BNS spin configurations. This template bank should contain as few templates as possible, while still being able to detect any BNS system that might be observed with aLIGO and AdV. To achieve this, it is important to assess the "effective dimension" of the space, which is defined as the number of orthogonal directions over which template waveforms need to placed in order to cover the full physically possible parameter range. We demonstrate that the effective dimension of this parameter space is only two dimensional. For BNS systems in aLIGO and AdV the extent of the physical parameter space in the remaining directions is smaller than the coverage radius of a template and can be neglected.

As the effective dimension of the space is two-dimensional, a hexagonal placement algorithm, similar to that used in previous searches of LIGO and Virgo data, could be employed to cover the space. This allows our new method to be incorporated into existing search pipelines in a straightforward way.

Since BNS systems coalesce at $\sim$ 1500 Hz, significantly higher than the most sensitive band of the detectors, the waveform will be dominated by the inspiral part of the signal [45]. The effect of component spin on BNS inspiral waveforms has been well explored in the literature [12–14, 41]). For spin-aligned (i.e. non-precessing) waveforms, the dominant effects of component spin are spin-orbit coupling, which enters the waveform phasing at 1.5PN order, and spin1-spin2 coupling, which enters the waveform phasing at 2PN order. Other spin-related corrections to the PN phasing have been computed [46, 47], however, in this work we mainly restrict to only the two dominant terms. The methods described here are easily extendable to include additional spin correction terms and this does not significantly change our results, as we demonstrate at the end of this section.

To construct a bank to search for generic BNS signals, we use TaylorF2 waveforms accurate to 3.5PN order in orbital phase and including the leading order spin-orbit and spin-spin terms given by [44, 45]

$$\tilde{h}(f) = A(f; \theta_x) e^{i\Psi(f; \lambda_i)} \tag{5}$$

where θ_x describe the various orientation angles that only affect the amplitude and overall phase of the observed gravitational waveform [24]. The phase Ψ is given by

$$\Psi = 2\pi f_0 x t_c - \phi_c + \lambda_0 x^{-5/3} + \lambda_2 x^{-1} + \lambda_3 x^{-2/3} + \lambda_4 x^{-1/3} + \lambda_{5L} \log(x) + \lambda_6 x^{1/3} + \lambda_{6L} \log(x) x^{1/3} + \lambda_7 x^{2/3}, \tag{6}$$

where f is the frequency, f_0 is a fiducial frequency, $x = f/f_0$, t_c is the coalescence time, ϕ_c is a constant phase offset. The PN phasing terms are

$$\lambda_0 = \frac{3}{128}(\pi\mathcal{M}f_0)^{-5/3}, \tag{7}$$

$$\lambda_2 = \frac{5}{96\eta^{2/5}}\left(\frac{743}{336} + \frac{11}{4}\eta\right)(\pi\mathcal{M}f_0)^{-1}, \tag{8}$$

$$\lambda_3 = -\frac{3\pi}{8\eta^{3/5}}\left(1 - \frac{1}{4\pi}\beta\right)(\pi\mathcal{M}f_0)^{-2/3}, \tag{9}$$

$$\lambda_4 = \frac{15}{64\eta^{4/5}}\left(\frac{3058673}{1016064} + \frac{5429}{1008}\eta + \frac{617}{144}\eta^2 - \sigma\right)(\pi\mathcal{M}f_0)^{-1/3} \tag{10}$$

$$\lambda_{5L} = \frac{3}{128\eta}\left(\frac{38645\pi}{756} - \frac{65\pi}{9}\eta\right) \tag{11}$$

$$\lambda_6 = \frac{3}{128\eta^{6/5}}\left(\frac{11583231236531}{4694215680} - \frac{640\pi^2}{3} - \frac{6848}{21}\left(\gamma_E + \log 4 - \frac{1}{5}\log\eta + \frac{1}{3}\log(\pi\mathcal{M}f_0)\right)\right.$$
$$\left. - \frac{15737765635}{3048192}\eta + \frac{2255\pi^2}{12}\eta + \frac{76055}{1728}\eta^2 - \frac{127825}{1296}\eta^3\right)(\pi\mathcal{M}f_0)^{1/3} \tag{12}$$

$$\lambda_{6L} = -\frac{1}{128\eta^{6/5}}\frac{6848}{21}(\pi\mathcal{M}f_0)^{1/3} \tag{13}$$

$$\lambda_7 = \frac{3}{128\eta^{7/5}}\left(\frac{77096675\pi}{254016} + \frac{378515\pi}{1512}\eta - \frac{74045\pi}{756}\eta^2\right)(\pi\mathcal{M}f_0)^{2/3}, \tag{14}$$

where γ_E is the Euler gamma constant, β (the dominant spin-orbit coupling term) and σ (the dominant spin-spin coupling term) are given by

$$\beta = \frac{1}{12}\sum_{i=1}^{2}\left[113\left(\frac{m_i}{m_1 + m_2}\right)^2 + 75\eta\right]\hat{\boldsymbol{L}} \cdot \boldsymbol{\chi}_i \tag{15}$$

$$\sigma = \frac{\eta}{48}\left(-247\boldsymbol{\chi}_1 \cdot \boldsymbol{\chi}_2 + 721\hat{\boldsymbol{L}} \cdot \boldsymbol{\chi}_1\hat{\boldsymbol{L}} \cdot \boldsymbol{\chi}_2\right). \tag{16}$$

and $\hat{\boldsymbol{L}}$ is the unit vector in the direction of the orbital angular momentum. Note that above we have omitted the λ_5 term, as it has no dependance on frequency and is therefore included in the constant phase offset, ϕ_c.

Our goal is to construct a template bank containing the minimum number of waveforms for which any plausible BNS signal has a FF of 0.97 or higher. To place a template bank, we follow the method of Owen [48]. We first construct a metric on the waveform parameter space that describes the mismatch between infinitesimally separated points,

$$\mathcal{O}(h(\boldsymbol{\theta}), h(\boldsymbol{\theta} + \delta\boldsymbol{\theta})) = 1 - \sum_{ij}g_{ij}(\boldsymbol{\theta})\,\delta\theta^i\,\delta\theta^j, \tag{17}$$

with the metric given by,

$$g_{ij}(\boldsymbol{\theta}) = -\frac{1}{2}\frac{\partial^2\mathcal{O}}{\partial\delta\theta^i\partial\delta\theta^j} = \left(\frac{\partial h(\boldsymbol{\theta})}{\partial\theta^i}\bigg|\frac{\partial h(\boldsymbol{\theta})}{\partial\theta^j}\right) \tag{18}$$

and where $\boldsymbol{\theta}$ describes the parameters of the signal, in this case the masses and the spins.

This metric is used to approximate the mismatch in the neighborhood of any point. When doing this care must be taken to choose a "good" set of coordinates where extrinsic curvature is minimized. If a "bad" set of coordinates is chosen, the region in which this approximation can be used will be very small. To minimize this issue when placing the two-dimensional non-spinning bank, the masses m_1, m_2 are transformed into the "chirp times" τ_0, τ_3 [25]. In this coordinate system, ellipses are constructed that describe fitting factors greater than 0.97 around a point and hexagonal placement is used to efficiently tile the space to achieve the desired minimal match [31].

To construct our new bank, we treat the six λ_i and two λ_{iL} components, given in Eq. (7), as eight independent parameters, as in [49]. The range of possible physical values will trace out a four-dimensional manifold in the eight dimensional parameter space given by the λ_α, where α is an index that takes both i and iL values. We will demonstrate that this eight-dimensional parameter space allows us to construct a metric without intrinsic curvature.

As shown in [48] it is possible to evaluate the derivative in (18), maximizing over the phase, ϕ_C, to give the metric in terms of a 9 dimensional space:

$$\gamma_{\alpha\beta} = \frac{1}{2}\left(\mathcal{J}[\psi_\alpha\psi_\beta] - \mathcal{J}[\psi_\alpha]\mathcal{J}[\psi_\beta]\right). \tag{19}$$

In this expression ψ_α is given by

$$\psi_0 = \frac{\partial \Psi}{\partial t_c} = 2\pi f_0 x \qquad (20)$$

$$\psi_i = \frac{\partial \Psi}{\partial \lambda_i} = x^{(i-5)/3} \qquad (21)$$

$$\psi_{iL} = \frac{\partial \Psi}{\partial \lambda_{iL}} = x^{(i-5)/3} \log(x) \qquad (22)$$

and $\mathcal{J}$ is the moment functional of the noise PSD [44, 48]

$$\mathcal{J}[a(x)] = \frac{1}{I(7)} \int_{x_L}^{x_U} \frac{a(x)x^{-7/3}}{S_h(xf_0)} \mathrm{d}x \ , \qquad (23)$$

where

$$I(q) \equiv \int_{x_L}^{x_U} \frac{x^{-q/3}}{S_h(xf_0)} \mathrm{d}x \qquad (24)$$

and x_U and x_L correspond to the lower and upper bounds of frequency in the integral. Unless stated otherwise we use $f_L = x_L f_0 = 15\text{Hz}$ for the aLIGO PSD and choose 2000Hz for the upper frequency cutoff, $f_U = x_U f_0$. While it is unphysical to use the same upper frequency cutoff for all systems, especially as we are not including a merger in our waveform model, it is necessary to make this assumption to ensure that our metric will be flat. For BNS systems this approximation is fair to use as such systems will merge at frequencies that are outside the sensitive range of the advanced detectors and thus our calculation of signal power is not affected by assuming that all BNS systems merge abruptly at 2000Hz. This approach was also used in [31] for computational efficiency.

Following [48] we can then maximize this expression over t_C to give the metric in terms of the eight λ_α

$$g_{\alpha\beta} = \gamma_{\alpha\beta} - \frac{\gamma_{0\alpha}\gamma_{0\beta}}{\gamma_{00}}. \qquad (25)$$

It is worth highlighting that the parameter space metric $g_{\alpha\beta}$, in the λ_α coordinate system, has no dependence on the values of λ_α. In other words, the parameter space is globally flat in this eight-dimensional parameter space.

Although this eight-dimensional metric is globally flat, we have increased the dimensionality of the physical waveform space by a factor of two. However, we can transform this metric to a new coordinate system that will allow us to assess the effective dimensionality of the parameter space. We first rotate and rescale the metric to transform to a Cartesian coordinate system. We now use indicies i, j to number the remaining eight λ_α coordinates. As g_{ij} is a real, symmetric matrix we can use the eigenvalues and eigenvectors of the metric to rotate into an orthonormal coordinate system defined by

$$\mu_i = \sum_j \left(V_{ij} \sqrt{E_i} \right) \lambda^j, \qquad (26)$$

where V_{ij} describes the eigenvectors of g_{ij} and E_i its corresponding eigenvalues. We use the convention that V_{ij} is the jth component of the ith eigenvector, and the eigenvectors are normalized by $V^T V = \mathcal{I}$. In this coordinate system,

the metric, g'_{ij}, will be the identity matrix. Next, we perform a rotation to align the axis of the parameter space with the principal components of the physically possible region of the space. The physically allowed ranges of the masses and spins cover only a limited region in the parameter space. The extent of the physically relevant region of the space in a certain direction may be thin relative to the desired mismatch. By orienting the coordinate system along the principal directions we can easily identify any orthogonal directions in which the physical region is sufficiently thin that we do not need to place templates in those directions. This will allow us to assess the effective dimension of the parameter space, or, in other words, how many directions we need to consider when placing a template bank. Transforming to a Cartesian coordinate system also helps with template placement, as it is trivial to place templates using the optimal A_n^* lattice [50] in a 2, 3 or 4 dimension Cartesian coordinate system

To perform the second rotation we make use of the fact that in a Cartesian coordinate system we are free to rotate the coordinates without changing the form of the metric. We would like to rotate the coordinates so that the greatest extent of the template bank lies along as few directions as possible. To accomplish this we first draw many examples of physical parameters of the masses and spins, and calculate the corresponding values of μ_i for each of these points. We then do a Principal Component Analysis on this dataset, which amounts to finding the eigenvectors of the covariance matrix from the set of μ_i. This produces a rotation into a new set of coordinates given by

$$\xi_i = \sum_j \left(C_{ij} \mu^j \right), \qquad (27)$$

where C_{ij} contains the eigenvectors of the covariance matrix using the same conventions as for V_{ij}. The rotation of course leaves the metric Cartesian, but now the bank is oriented along the principal axes and it is much easier to visualize the shape of the boundaries and determine how to perform the template placement.

We now use this method to construct a template bank where the spin of each component neutron star is restricted to 0.4. When this metric is constructed using the aLIGO, zero-detuned high-power noise curve with a lower frequency cut-off of 15Hz we show that, although many additional templates are required to cover an aligned spinning parameter space when compared to the non spinning space, the effective dimension for these BNS systems is still two.

We begin by attempting to visualize the space. We will refer to ξ_1 as the direction along which the parameter space has the biggest extent (the dominant direction) and ξ_8 as the direction with the smallest extent (the least-dominant direction). We draw a large set of points, with random values of masses and spins, and transform these points into the ξ_i coordinate system. The position of these points is shown in Figure 2, where we plot the extent of $\xi_{2,3,4}$ against ξ_1.

In Figure 2 and subsequent plots, we have scaled the ξ_i direction such that one unit corresponds to the coverage diameter of a template at 0.97 mismatch. Equivalently, we have scaled the directions such that two points separated by 0.5
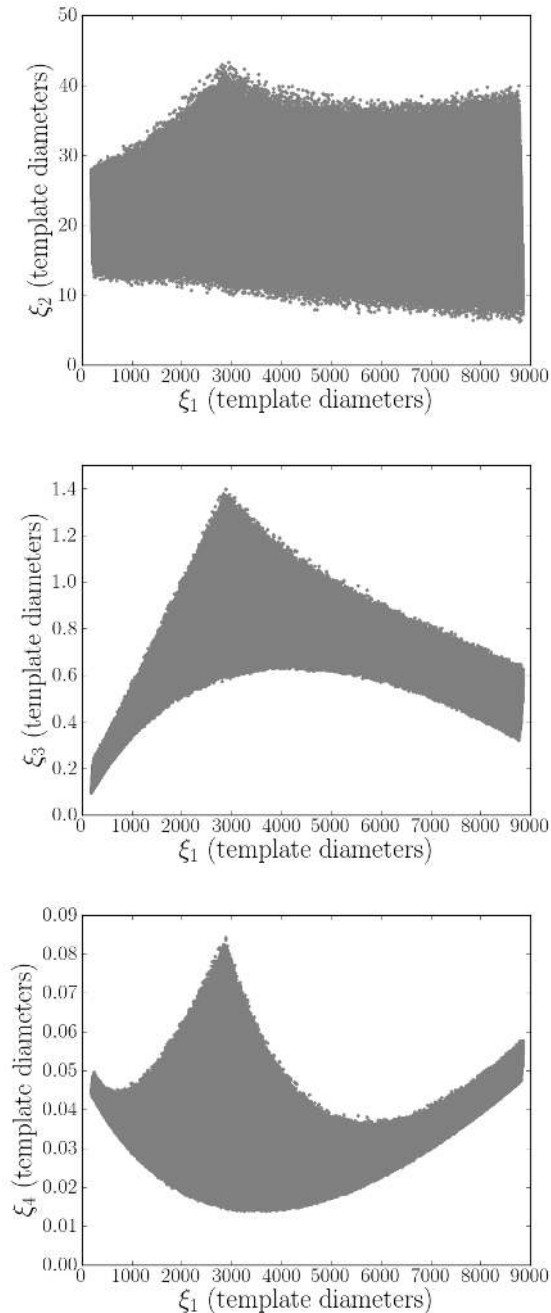
FIG. 2. The extent of the binary neutron star, $\chi_i < 0.4$, parameter space in the ξ_2, ξ_3 and ξ_4 directions, plotted against ξ_1. The ξ_i coordinates have been scaled such that one unit corresponds to the coverage diameter of a template at 0.97 mismatch. Generated using the zero-detuned, high-power advanced LIGO sensitivity curve with a 15Hz lower frequency cut off.

units (one template radius) in any direction have a match of 0.97[1]. We remind that mismatch is proportional to distance

squared and therefore two points separated by one unit would have a match of 0.88

Immediately we notice that the extent along the ξ_4 direction is small compared to the diameter of a template. We can also see that the extent along the ξ_3 direction is comparable to a template diameter, while the ξ_1 and ξ_2 directions have much larger extents and clearly need to be gridded over. The extent in the other 4 directions is smaller than ξ_4 and can be completely ignored. This hierarchy of measurable parameters may be a generic feature according to the model of [51].

The plot of ξ_1 against ξ_3 in Figure 2 can be somewhat misleading as we have projected out the ξ_2 direction. It is more informative to investigate the depth of ξ_3 at fixed values of ξ_1 and ξ_2 and translate this into the maximum mismatch that would be obtained if one were to assume that there is no width in the third direction. In Figure 3 we show the maximum mismatch between the central and extremal values of the possible range of ξ_3 (and ξ_4) as a function of the two primary directions. This is calculated by binning the points mentioned above into bins in ξ_1 and ξ_2, where the bin width is equal to one template radius. We then determine the extremal values of ξ_3 (and ξ_4) for the points in each bin. From Figure 3 we can see that, while there are small areas of parameter space where up to a 1.6% loss in SNR would be incurred from assuming the ξ_3 direction had no depth, most areas of the parameter space are very thin in the ξ_3 direction. This figure also helps to reinforce the fact that the depth in the fourth direction is negligible, as, even in the worst region of the space, no more than 0.01% of SNR would be lost by assuming ξ_4 had no depth. The depth of the $\xi_{5..8}$ directions are even smaller than ξ_4.

In this coordinate system it is easy to explore how the size of the parameter space depends on the maximal spins of the component neutron stars. In Figure 4 we show the extent of the physical space for aligned spinning BNS systems, with maximum component spins of 0.4, 0.2 and 0.1, compared to that of non-spinning systems. Ignoring any issues related to the depth of the ξ_3 direction, one can clearly see that to cover the aligned spin parameter space will require a great deal more templates than the non spinning parameter space.

From these results we can see that a 2 dimensional template bank would be sufficient to cover the aligned spin parameter space for BNS systems in the advanced detector era. Specifically, we would advocate placing a hexagonal lattice in the ξ_1, ξ_2 coordinates and setting the value of $\xi_{3..8}$ to be the middle of the possible range of those parameters at the given position of ξ_1, ξ_2. For the regions of parameter space where the depth of ξ_3 is not negligible, one could either ignore it, understanding that the resulting bank will not have a fitting factor of 0.97 in this region. Alternatively, one could stack templates in the region where ξ_3 is deepest to minimize this effect.

For this work we chose to employ a hexagonal template bank in the ξ_1, ξ_2 coordinates, stacking the templates in the ξ_3 direction, where necessary, to ensure that the maximum mismatch due to the depth of ξ_3 is no more than 0.25%. For

[1] The unscaled distance between two points with a match of 0.97 would be
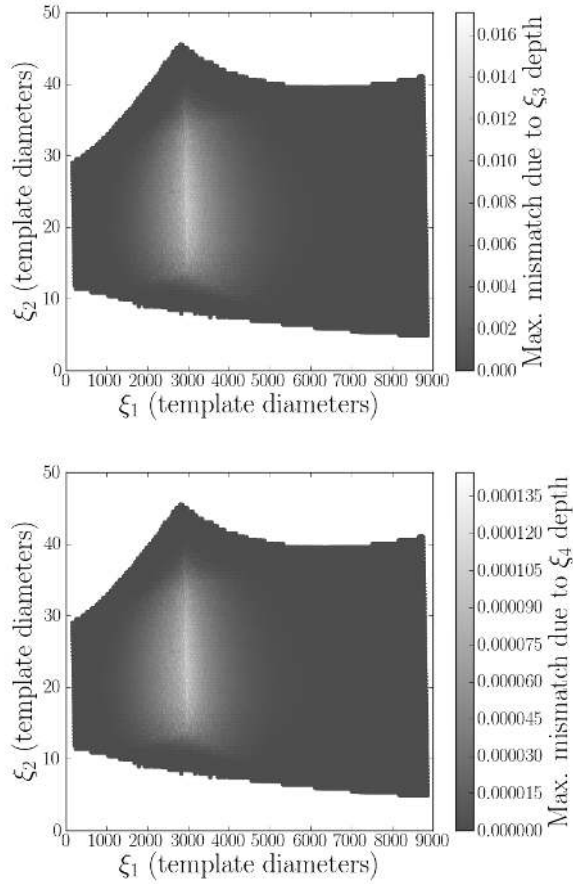
$(1 - 0.97)^{0.5} = 0.17$

FIG. 3. The mismatch between the edge and centre of the physically possible range of ξ_3 (top) and ξ_4 (bottom) values as a function of ξ_1 and ξ_2. The ξ_i coordinates have been scaled such that one unit corresponds to the coverage diameter of a template at 0.97 mismatch. Plotted for a binary neutron star parameter space with spins restricted to 0.4 using the zero-detuned, high-power advanced LIGO sensitivity curve with a 15Hz lower frequency cut off.
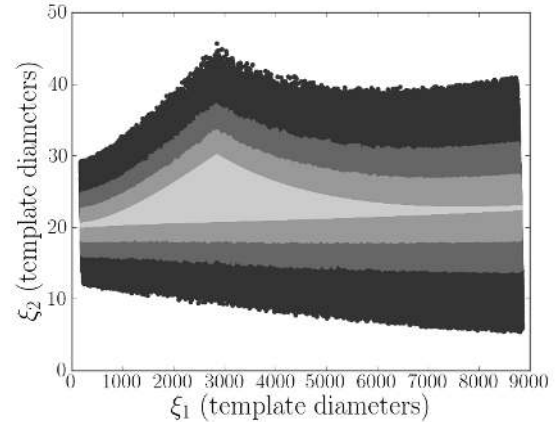

FIG. 4. The size of the BNS parameter space as a function of the maximum spin. The darkest points indicate points with spin on both components constrained to 0.4, then, in order of increasing lightness, we show points constrained to a maximal spin of 0.2 and 0.1, finally the lightest points show points with no spin. The ξ_i coordinates have been scaled such that one unit corresponds to the coverage diameter of a template at 0.97 mismatch. This plot was generated using the zero-detuned, high-power aLIGO sensitivity curve with a 15Hz lower frequency cut off.
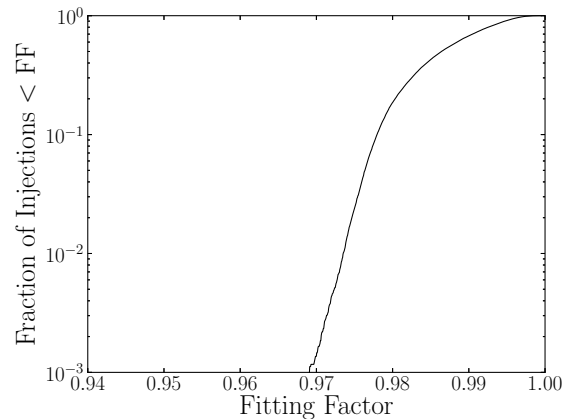

FIG. 5. The distribution of fitting factors obtained by searching for aligned spin, binary neutron star systems, with spin magnitudes restricted to 0.4 using the aligned-spin BNS template bank described in section III and the aLIGO, zero-detuned, high-power PSD with a 15Hz lower frequency cutoff.

an aligned-spin template bank where the spin of each component is restricted to 0.4, using the advanced LIGO, zero-detuned high-power noise curve with a lower frequency cut-off of 15Hz, we find that approximately 520,000 templates are required. Roughly 100,000 of these templates were added by the stacking process.

We can verify that the template bank algorithm is working correctly by repeating the simulation described in section II, but evaluating the fitting factor between our bank of aligned-spin template waveforms and a set of signals that is restricted to having spins that are (anti-)aligned with the orbital angular momentum. The results of this simulation are shown in figure 5 and one can see that with our bank we do not observe fitting factors lower than 0.97 when searching for aligned spin BNS systems.

In the previous paragraphs we have restricted attention to the aLIGO zero-detuned, high-power predicted sensitivity with a 15Hz lower frequency cut off. However, we should verify that the conclusions we have drawn are valid for AdV,

whose PSD is different from that of aLIGO, as shown in Figure 6. Additionally we should also show that the choice to use a 15Hz cut off in the aLIGO PSD does not affect the conclusions made in this section.

The process we described above is applicable for any PSD, and therefore we can use it directly to determine the ξ_i directions for the AdV PSD, or the aLIGO PSD with a 10Hz lower frequency cutoff. In Figure 7 we plot ξ_1 against ξ_2 for both PSDs while the color shows the mismatch between the center and edges in the ξ_3 direction. This plot can be directly
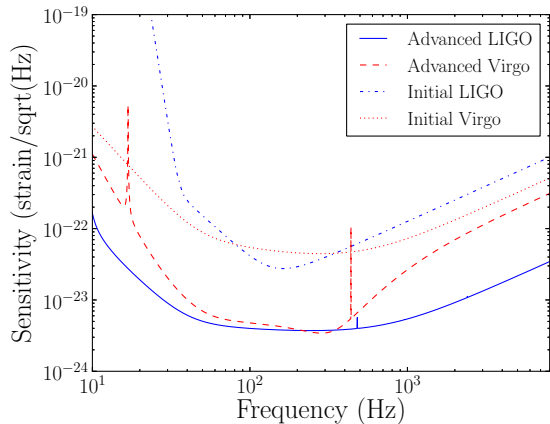
FIG. 6. The amplitude spectral density for the aLIGO zero-detuned high-power design sensitivity (blue solid curve), AdV design sensitivity (red dashed curve), initial LIGO design sensitivity (blue bot-dash curve) and initial Virgo design sensitivity (red dotted curve).

compared to Figure 3. We notice that the size of the parameter space for the AdV PSD is significantly smaller than for the aLIGO PSD in all 3 of the dominant directions. Therefore our conclusions for aLIGO are still valid for AdV. Using our method we find that we require approximately 120,000 templates to cover the parameter space for AdV, in comparison to approximately 520,000 templates for aLIGO.

By comparing the results when using the aLIGO PSD with a 10Hz and 15Hz lower cut off we observe that using a 10Hz lower frequency cut off will increase the number of necessary templates from ~ 520000 to ~ 860000. However the shape of the parameter space, and thus our final conclusions, are unaffected when using a 10Hz lower frequency cutoff. However, in this case we see larger mismatches due to the depth of ξ_3 and therefore the process of stacking templates is important when using a 10Hz lower cut off. However, even in this case, we do not feel that the depth is large enough everywhere in the space to justify using a fully 3-dimensional placement algorithm.

Finally, we wish to investigate the effect that the higher order spin contributions to the orbital phase have on our method. To do this we repeat the process described above, but include the spin(1)-spin(1) and spin(2)-spin(2) contributions to the σ term at 2PN order and also the 2.5PN spin-orbit term as given in [47]. In Figure 8 we plot ξ_1 against ξ_2 when these higher order spin terms are included, the color shows the mismatch between the center and edges in the ξ_3 direction. This plot can be directly compared to Figure 3. By comparing these plots we can see that including the higher order spin terms has caused the parameter space to have a larger extent in the ξ_2 direction. However, the depth of the space in the ξ_3 direction has reduced by almost an order of magnitude. In this case the stacking process is not required and the resulting bank consists of ~ 560000 templates.
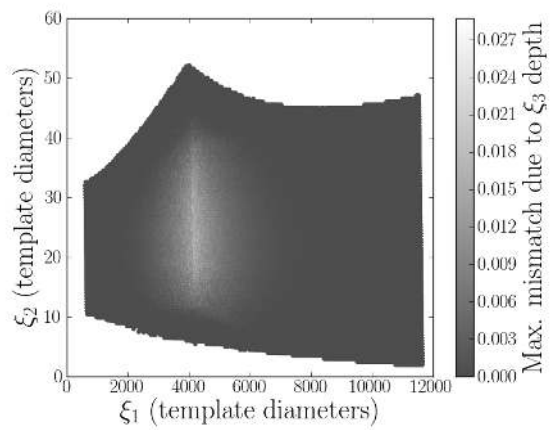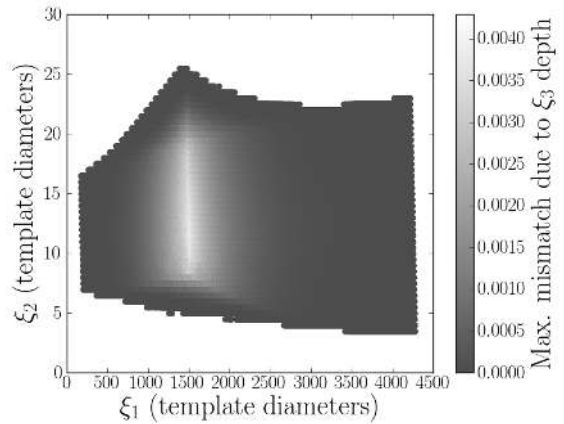

FIG. 7. The mismatch between the edge and centre of the third dominant direction as a function of the first and second dominant directions when using the Virgo noise curve (top) and when using the advanced LIGO noise curve with a 10Hz lower frequency cut off (bottom). The ξ_i coordinates have been scaled such that one unit corresponds to the coverage diameter of a template at 0.97 mismatch. Plotted for a binary neutron star parameter space with spins restricted to 0.4.

IV. COMPARISON TO ALTERNATIVE PLACEMENT METHODS

An alternative approach to template placement for aligned spin systems is to use templates with "unphysical" values of the symmetric mass ratio, η. That is, to use non-spinning templates, with the desired range of chirp mass but where the range of η values is extended to include both values of η that are much lower than the relevant parameter space and values of η that are much higher, including templates with η greater than the physically possible limit of 0.25.

We can understand this unphysical η approach in terms of our ξ_i coordinate system by noting that it is always possible to produce a template with any possible value of ξ_1 and ξ_2 that is within the BNS parameter space, by using non-spinning templates with unrestricted values of η. By generating a set of templates in the ξ_1, ξ_2 directions, where we restrict the chirp mass to be that possible for BNS systems, but where η ranges
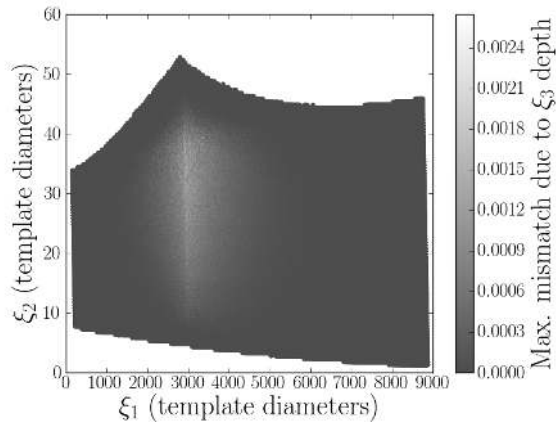
FIG. 8. The mismatch between the edge and centre of the third dominant direction as a function of the first and second dominant directions using waveforms incorporating the sub-dominant spin corrections to the orbital phase. The ξ_i coordinates have been scaled such that one unit corresponds to the coverage diameter of a template at 0.97 mismatch. Plotted for a binary neutron star parameter space with spins restricted to 0.4 using the zero-detuned, high-power aLIGO sensitivity curve with a 15Hz lower frequency cut off.
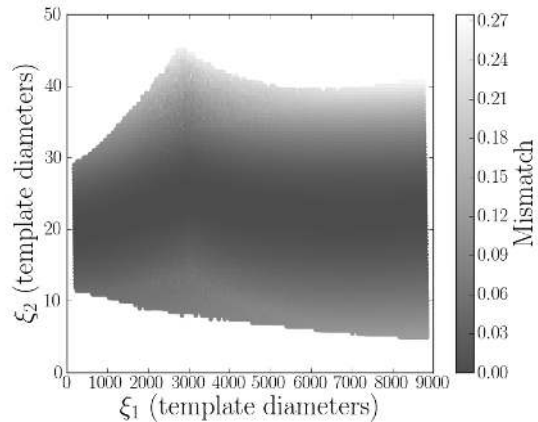

FIG. 9. The mismatch between unphysical η and aligned spin BNS templates as a function of the first and second dominant directions. In making this plot we assume that ξ_3 has no depth in the aligned spin case by taking the central value where ξ_3 has a range of values. This plot was generated with spins restricted to 0.4 using the zero-detuned, high-power advanced LIGO sensitivity curve with a 15Hz lower frequency cut off.

from 0.1 to 0.7 we are able to cover the full physically possible space in ξ_1, ξ_2. However, the disadvantage to using unphysical η templates is that the points will not take the correct values of ξ_3. The colorbar on Figure 9 indicates the mismatch between unphysical η templates and aligned-spin templates as a function of ξ_1 and ξ_2. In making this plot we assume that ξ_3 has no depth in the aligned spin case by taking the central value where ξ_3 has a range of values.

While unphysical η templates will produce an increase in efficiency when compared with non-spinning templates, the method is not as efficient as the aligned spin geometrical placement we have described. In addition, both methods require the same number of templates to cover the parameter space. Therefore, we would recommend using aligned spin templates placed using our metric algorithm as opposed to unphysical η templates.

Finally, we wish to compare the performance of this geometrical algorithm with the stochastic bank proposed in [32, 52]. The stochastic placement works by randomly placing points within the parameter space and rejecting points that are too "close" to points already in the bank. This has the advantage that it is valid for any parameter space metric, so we could use any of the metrics discussed above. However, it is more computationally efficient to use the Cartesian ξ_i or μ_i coordinate system rather than the non-Cartesian metric given above.

The disadvantage to a stochastic bank, when compared to a geometrically placed bank, is that it will require more templates to achieve the same level of coverage [32, 53]. For our parameter space, consisting of BNS signals with component spins up to 0.4 and using the advanced LIGO zero-detuned high-power design curve with a 15Hz lower frequency cut-off, we found that the stochastic placement produced a bank con-

taining ~ 750000 templates, which is 44% more than with the geometrical placement. However, stochastic placement can still be used to place templates when no analytical metric is known, such as when the merger becomes important. In such regions of parameter space, the stochastic placement may still be the best algorithm to use to place a template bank.

V. PERFORMANCE OF THE ALIGNED SPIN TEMPLATE BANK

In this section we would like to investigate the improvement in the detection of generic BNS systems that results from using a template bank that includes the dominant, non-precessing, spin effects. To do this we use the aligned spinning bank that we detail in section III and compare this to the results of using a nonspinning bank as shown in section II.

Using our aligned spin template bank, we repeat the investigation from section II. We create a population of source BNS signals identical to those used in II, and compute the fitting factor between these signals and the aligned spin template bank. The results of this are shown in FIG.10. To decrease the computational cost of this test, we only calculated the overlaps between a signal and templates that were within a range of $\pm 0.1 M_\odot$ in chirp mass. This is reasonable because the overlap will decrease rapidly with small changes in chirp mass, therefore we expect templates with very different values of chirp mass to have low overlaps with each other. We verified that this approach did not cause us to underestimate the fitting-factor of our banks.

We can now compare the results obtained in this section, using our aligned-spin template bank, with the results obtained in section II, using a non-spinning template bank. One can clearly see an improvement in the distribution of fitting fac-
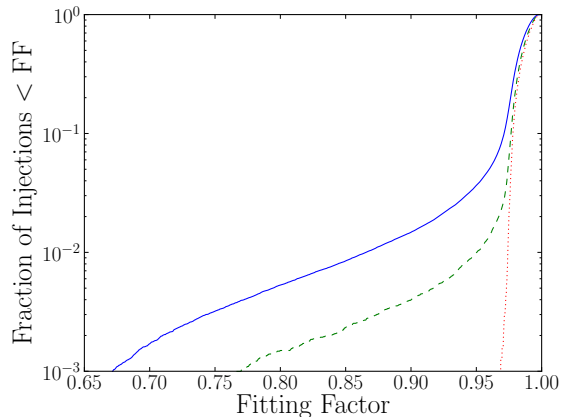
FIG. 10. The distribution of fitting factors obtained by searching for the precessing signals described in section II with component spins up to 0.4 (blue solid line), 0.2 (green dashed line), and 0.05 (red dotted line) using the aligned spin BNS template bank described in section III and the advanced LIGO, zero-detuned, high-power PSD with a 15Hz lower frequency cutoff.
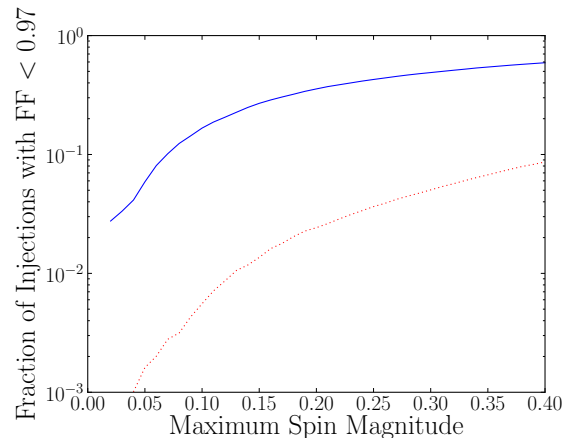

FIG. 11. The fraction of the precessing signals described in section II recovered with a fitting factor less than 0.97 as a function of the maximum component spin. Shown for the non-spinning BNS template bank described in section II (blue solid line), and the aligned spin BNS template bank described in section III (red dotted line). The advanced LIGO, zero-detuned, high-power PSD with a 15Hz lower frequency cutoff was used when computing the fitting factors.

tors when using the aligned spin template bank. The fraction of signals that fall below a fitting factor of 0.97, when the spin magnitudes are restricted to 0.4, falls from 59% to 9%. We also see an improvement for signals that have spin magnitudes restricted to 0.05, where the fraction of signals falling below a fitting factor of 0.97 drops from 6% to 0.2%. We can also compare the performance of the aligned-spin bank to that of the non-spinning bank as a function of the maximum spin magnitude, as shown in Figure 11. From this Figure we can see that regardless of the maximum component spin, the aligned spin bank will greatly reduce the number of signals recovered with fitting factors less than 0.97.

A small fraction of signals fall below a FF of 0.97, even when using the new aligned-spin template bank. We expect that these poor matches with the aligned template bank are due to precession. In general, precessional effects will not be important in BNS systems as the orbital angular momentum is significantly larger than the component spins. In such cases there is only a small angle between the total and orbital angular momenta and precession has only a small effect on the waveform.

However, there is a small region of parameter space where precessional effects *will* have an effect for BNS systems. Using the model of Ref. [54], applied to the small precession angles in BNS systems, we can predict for which systems precession will be most important. The orientation of a precessing binary must be defined using the total angular momentum rather than the orbital angular momentum as done with non-precessing binaries. The orientations with the worst matches should be those where the system is edge-on (angular momentum perpendicular to the viewing direction) and where the detector is nearly insensitive to the plus polarization and only sees the cross polarization (a binary overhead of the detector would have its angular momentum oriented $45°$ between the arms of the detector). We find that this is indeed the case; in

fact, all cases with fitting factors less than 0.95 are close to this configuration. All of these cases also have biases in the recovered mass and spin parameters due to the secular effects of precession on the phasing of the waveform.

VI. CONCLUSION

In this work we have investigated the effects of neglecting spin when searching for binary neutron star systems in aLIGO and AdV. We have found that, if component spins in binary neutron star systems are as large as 0.4, then neutron star spin cannot be neglected, and there is a non-trivial loss in signal-to-noise ratio even if the maximum spin is restricted to be less than 0.05. We have developed a new algorithm for placing an aligned spin template bank in the BNS parameter space. We have shown that this bank works for aligned spin systems and have demonstrated that it does significantly better for generic, precessing BNS systems than the traditional non-spinning bank. However, for the BNS aligned spin $\chi_i < 0.4$ parameter space the aligned spin bank requires approximately five times as many templates as the non-spinning bank. This increased number of templates will increase the computational cost of the search and increase the number of background events, so needs to be balanced against the potential gain in being able to cover a larger region of parameter space. A further advantage of our method is the ease with which it can be incorporated into existing or future search pipelines, which include the use of signal-based vetoes [55] and coincidence algorithms [56]. In future work we will investigate how this template bank performs in data from the aLIGO and AdV detectors which includes non-Gaussian and non-stationary noise features. Finally we note that the method proposed in this work should be applicable wherever the Tay-

lorF2 waveforms closely represent actual gravitational waveforms. In a future work we will investigate how well this method performs in the binary black hole and neutron-star, black-hole regions of the parameter space. Wherever the TaylorF2 approximation begins to break down, a stochastic bank placement may still be the most viable option.

[1] G. M. Harry *et al.*, Class. Quant. Grav. **27**, 084006 (2010).
[2] F. Acernese *et al.*, (2009), Virgo Technical Report 0027A-09.
[3] J. Abadie *et al.*, Class.Quant.Grav. **27**, 173001 (2010).
[4] L. Blanchet, Living Rev.Rel. **9** (2006).
[5] P. C. Peters and J. Mathews, Phys. Rev. **131**, 435 (1963).
[6] L. Blanchet, T. Damour, and B. R. Iyer, Phys. Rev. **D51**, 5360 (1995).
[7] L. Blanchet, T. Damour, B. R. Iyer, C. M. Will, and A. G. Wiseman, Phys. Rev. Lett. **74**, 3515 (1995).
[8] L. Blanchet, B. R. Iyer, C. M. Will, and A. G. Wiseman, Class. Quantum Grav. **13**, 575 (1996).
[9] A. G. Wiseman, Phys. Rev. D **48**, 4757 (1993).
[10] L. Blanchet, G. Faye, B. R. Iyer, and B. Joguet, Phys. Rev. D **65**, 061501(R) (2002), Erratum-ibid **71**, 129902(E) (2005).
[11] L. Blanchet, T. Damour, G. Esposito-Farese, and B. R. Iyer, Phys. Rev. Lett. **93**, 091101 (2004).
[12] L. E. Kidder, C. M. Will, and A. G. Wiseman, Phys. Rev. **D47**, 4183 (1993).
[13] T. A. Apostolatos, C. Cutler, G. J. Sussman, and K. S. Thorne, Phys. Rev. **D49**, 6274 (1994).
[14] L. E. Kidder, Phys. Rev. **D52**, 821 (1995).
[15] L. Blanchet, A. Buonanno, and G. Faye, Phys.Rev. **D74**, 104034 (2006).
[16] K.-W. Lo and L.-M. Lin, Astrophys.J. **728**, 12 (2011).
[17] D. Lorimer, Living Rev.Rel. **11**, 8 (2008).
[18] I. Mandel and R. O'Shaughnessy, Class. Quant. Grav. **27**, 114007 (2010).
[19] L. Bildsten *et al.*, Astrophys J. Supp. **113**, 367 (1997).
[20] D. Chakrabarty, AIP Conference Series American Institute of Physics Conference Series, **1068**, 67 (2008).
[21] M. Burgay *et al.*, Nature **426**, 531 (2003).
[22] J. Grindlay, S. P. Zwart, and S. McMillan, Nature Physics **2**, 116 (2006).
[23] W. M. Farr *et al.*, Astrophys.J. **742**, 81 (2011).
[24] B. Allen *et al.*, (2005), arXiv:gr-qc/0509116 [gr-qc].
[25] B. J. Owen and B. S. Sathyaprakash, Phys. Rev. **D60**, 022002 (1999).
[26] F. Marion *et al.* (Virgo Collaboration), in *Proceedings of the Rencontres de Moriond 2003* (2004).
[27] K. Cannon *et al.*, Phys.Rev. **D82**, 044025 (2010).
[28] J. Abadie *et al.*, Phys.Rev. **D85**, 082002 (2012).
[29] T. A. Apostolatos, Phys.Rev. **D54**, 2421 (1996).
[30] P. Ajith, Phys.Rev. **D84**, 084037 (2011).

[31] S. Babak *et al.*, Class. Quant. Grav. **23**, 5477 (2006).
[32] I. W. Harry, B. Allen, and B. S. Sathyaprakash, Phys. Rev. **D80**, 104014 (2009).
[33] T. A. Apostolatos, Phys.Rev. **D52**, 605 (1995).
[34] C. Cutler and E. E. Flanagan, Phys. Rev. D **49**, 2658 (1994).
[35] C. Cutler *et al.*, Phys. Rev. Lett. **70**, 2984 (1993).
[36] S. Droz, D. J. Knapp, E. Poisson, and B. J. Owen, Phys. Rev. D **59**, 124016 (1999).
[37] T. Cokelaer, Phys. Rev. **D76**, 102004 (2007).
[38] B. P. Abbott *et al.* (LIGO Scientific Collaboration), Phys. Rev. **D79**, 122001 (2009), arXiv:0901.0302 [gr-qc].
[39] B. P. Abbott *et al.* (LIGO Scientific Collaboration), Phys. Rev. **D80**, 047101 (2009), arXiv:0905.3710 [gr-qc].
[40] J. Abadie *et al.* (LIGO and Virgo Scientific Collaborations), Phys. Rev. **D82**, 102001 (2010), arXiv:1005.4655 [gr-qc].
[41] A. Buonanno, Y. Chen, and M. Vallisneri, Phys. Rev. D **67**, 104025 (2003), erratum-ibid. **D** 74, 029904(E) (2006), gr-qc/0211087.
[42] "LSC Algorithm Library Suite," `https://www.lsc-group.phys.uwm.edu/daswg/projects/lalsuite.html`.
[43] B. Abbott *et al.* (LIGO Scientific Collaboration), *Advanced LIGO anticipated sensitivity curves*, Tech. Rep. LIGO-T0900288-v3 (2010).
[44] E. Poisson and C. M. Will, Phys. Rev. D **52**, 848 (1995).
[45] A. Buonanno, B. R. Iyer, E. Ochsner, Y. Pan, and B. S. Sathyaprakash, Phys. Rev. **D80**, 084043 (2009), arXiv:0907.0700 [gr-qc].
[46] B. Mikoczi, M. Vasuth, and L. A. Gergely, Phys.Rev. **D71**, 124043 (2005), arXiv:astro-ph/0504538 [astro-ph].
[47] K. G. Arun, A. Buonanno, G. Faye, and E. Ochsner, Phys. Rev. **D79**, 104023 (2009), arXiv:0810.5336 [gr-qc].
[48] B. J. Owen, Phys. Rev. **D53**, 6749 (1996).
[49] A. Pai and K. Arun, (2012), arXiv:1207.1943 [gr-qc].
[50] J. Conway and N. Sloane, *Sphere Packings, Lattices and Groups*, 2nd ed. (Springer-Verlag, New York, 1993).
[51] M. K. Transtrum, B. B. Machta, and J. P. Sethna, Phys.Rev.Lett. **104**, 060201 (2010), arXiv:0909.3884 [cond-mat.stat-mech].
[52] S. Babak, Class. Quant. Grav. **25**, 195011 (2008), arXiv:0801.4070 [gr-qc].
[53] G. M. Manca and M. Vallisneri, Phys.Rev. **D81**, 024004 (2010), arXiv:0909.0563 [gr-qc].

[54] D. A. Brown, A. Lundgren, and R. O'Shaughnessy, (2012), arXiv:1203.6060.

[55] B. Allen, Phys. Rev. **D71**, 062001 (2005), arXiv:gr-qc/0405045.

[56] C. A. K. Robinson, B. S. Sathyaprakash, and A. S. Sengupta, Phys. Rev. **D78**, 062002 (2008), arXiv:0804.4816 [gr-qc].